

# Spectral evolution in (Ca,Sr)RuO<sub>3</sub> near the Mott-Hubbard transition

J. S. Ahn,<sup>1</sup> J. Bak,<sup>1</sup> H. S. Choi,<sup>1</sup> T. W. Noh,<sup>1,2</sup> J. E. Han,<sup>3</sup> Yunkyung Bang,<sup>4</sup> J. H. Cho,<sup>5</sup> and Q. X. Xia<sup>6</sup>

<sup>1</sup>*Department of Physics, Seoul National University, Seoul 151-742, Korea*

<sup>2</sup>*LG Corporative Institute of Technology, Seoul 137-140, Korea*

<sup>3</sup>*Max-Planck Institut für Festkörperforschung, Heisenbergstr. 1, D-70569, Stuttgart, Germany*

<sup>4</sup>*Department of Physics, Chonnam National University, Kwangju 500-757, Korea*

<sup>5</sup>*RCDAMP and Department of Physics, Pusan National University, Pusan 609-735, Korea*

<sup>6</sup>*Superconductivity Technology Center, Los Alamos National Laboratory, Los Alamos, NM 87545, USA*

We investigated the optical properties of (Ca,Sr)RuO<sub>3</sub> films on the borderline of a metal-insulator (M-I) transition. Our results show all of the predicted characteristics for a metallic Mott-Hubbard system, including (i) a mass enhancement in dc-limit, (ii) an  $U/2$  excitation, and (iii) an  $U$  excitation. Also, a self-consistency is found within the Gutzwiller-Brinkman-Rice picture for the Mott transition. Our finding displays that electron correlation should be important even in  $4d$  materials.

PACS numbers: 71.30.+h, 71.27.+a, 71.10.Fd, 78.20.-e

Correlation between electrons in transition and rare earth metal compounds has attracted lots of attentions. In general, the more localized the electron wave function is, the stronger the correlation effects are. As a result, correlation effects are believed to be much more important in describing  $3d$  electrons than  $4d$  or  $5d$  electrons.

A metal-insulator (M-I) transition driven by electron correlation was proposed by Mott and subsequently investigated intensively. [1] Since the Hubbard model was proposed in early 1960's, it has been widely accepted as the simplest model which can describe correlation effects. Although the model is composed of only two parameters, i.e. inter-site hopping energy  $t$  ( $= W/z$ ) and on-site Coulomb repulsive energy  $U$ , it has not been exactly solved yet except for one dimensional case. [ $W$  and  $z$  are the bandwidth and the coordination number, respectively.] Up to several years ago, different approaches provided limited insights into different aspects of the M-I transition. However, recent theoretical progresses, including a slave-boson approach, infinite dimension limit approaches with several techniques, and numerical calculations for finite size systems, started to provide a coherent picture. [2]

According to the traditional Gutzwiller-Brinkman-Rice (GBR) picture, [3] the Mott M-I transition from a metallic side can be described by narrowing and disappearing of a Fermi liquid quasi-particle (QP) band at a critical value of correlation strength,  $(U/W)_c$ . Under this strong renormalization, an effective mass,  $m^*$ , [4] of the QP is related by:

$$\frac{1}{m^*} = 1 - \frac{(U/W)^2}{(U/W)_c^2}. \quad (1)$$

Recent theoretical works predict that one particle spectral function  $A(\omega)$  for the metallic phase will be split into lower (LHB) and upper (UHB) Hubbard bands, in addition to the QP band located at zero frequency. Fig. 1(a) shows the schematic diagram of  $A(\omega)$ . Then, the corresponding optical conductivity spectra  $\sigma_1(\omega)$  can be

easily predicted and displayed in Fig. 1(b). Note that  $\sigma_1(\omega)$  in a metallic side has three pronounced features: (i) a "QP peak" near zero frequency, (ii) an " $U/2$  peak" due to optical transitions between QP band and LHB (or UHB), and (iii) an " $U$  peak" due to a transition between LHB and UHB.

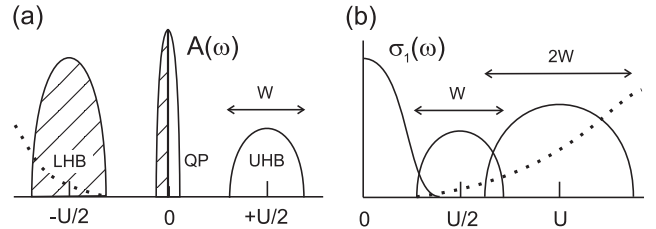


FIG. 1. Schematic diagrams of (a) one particle spectral function and (b) optical conductivity, for  $4/6$ -filled metallic Mott-Hubbard system. Dotted lines indicate the contributions from  $O(2p)$  band.

In this letter, we will report optical properties of (Ca,Sr)RuO<sub>3</sub> films, where four electrons occupy triply degenerate  $t_{2g}$  levels. It is widely accepted that some titanates and vanadates, which are usually approximated as half-filled cases of a single orbital, can be described by the Hubbard model. Most efforts to understand Mott-Hubbard physics have been focused on such  $3d$  oxides. [5,6] However, as far as we know, such  $3d$  oxides do not display all of the above-mentioned features for  $1/m^*$  and  $\sigma_1(\omega)$ , which are expected for an ideal Mott-Hubbard system. In ruthenates, there have been controversies between band and correlation pictures. [7-10] Surprisingly enough, we found that our (Ca,Sr)RuO<sub>3</sub> films, i.e. a  $4/6$ -filled  $4d$  electron system, displays the mass enhancement and the optical features due to correlation very clearly.

SrRuO<sub>3</sub> is known to be a bad metal which shows a ferromagnetic ordering at  $T_c \sim 160$  K. CaRuO<sub>3</sub> is also barely metallic, but it does not show any magnetic ordering down to 4.2 K. Since CaRuO<sub>3</sub> has a narrower bandwidth than SrRuO<sub>3</sub>, it stands on the borderline of M-I

transitions in ternary  $\text{Ru}^{4+}$  oxides. [11] Therefore, if epitaxial  $\text{CaRuO}_3$  thin films are fabricated, their electrical properties can be easily controlled from metal to insulator through strain effect. [12] Using this effect, we were able to prepare epitaxial  $(\text{Ca,Sr})\text{RuO}_3$  thin films, where the Ca substitution makes them closer to the M-I transition from metallic side.

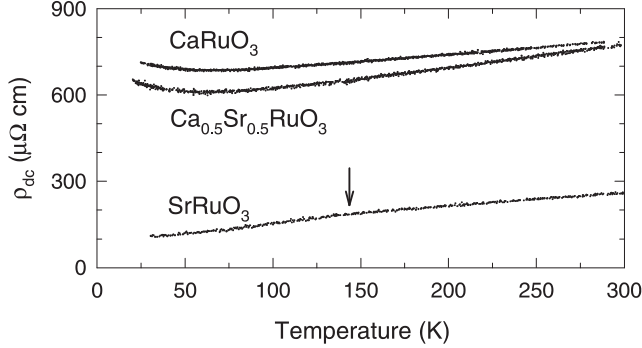


FIG. 2. Resistivity versus temperature for  $(\text{Ca,Sr})\text{RuO}_3$ . Arrow indicates the Curie temperature of  $\text{SrRuO}_3$ .

$(\text{Ca,Sr})\text{RuO}_3$  films were grown on single crystal  $\text{SrTiO}_3(100)$  substrates by pulsed laser deposition. [13] Fig. 2 shows the temperature dependent dc resistivity  $\rho_{dc}$  curves. The  $\text{SrRuO}_3$  film shows a metallic behavior with a small slope change around 140 K, which corresponds to its  $T_c$  value. Both of the  $\text{Ca}_{0.5}\text{Sr}_{0.5}\text{RuO}_3$  and the  $\text{CaRuO}_3$  films show barely metallic behaviors: their  $\rho_{dc}$  values are close to about  $1000 \mu\Omega \text{ cm}$ , which corresponds to the Mott minimum metallic conductivity. [1] The  $\rho_{dc}$  value of the  $\text{CaRuO}_3$  film is larger than its bulk value by a factor of 3, due to the strain effect.

To obtain accurate optical properties of  $(\text{Ca,Sr})\text{RuO}_3$  films in a wide frequency region of  $0.23 \sim 5.0 \text{ eV}$ , we combined reflectance and transmittance measurements with spectroscopic ellipsometry. [13] Between 0.23 and 3.0 eV,  $\sigma_1(\omega)$  were obtained accurately from reflectance and transmittance spectra using the Fresnel equations. Above 1.5 eV,  $\sigma_1(\omega)$  were determined by spectroscopic ellipsometry. In these methods, any extrapolation procedures, which are commonly used in the Kramers-Kronig analysis of reflectance spectra, [14] were not required.

Figure 3(a) shows  $\sigma_1(\omega)$  of the  $(\text{Ca,Sr})\text{RuO}_3$  films. Below  $\sim 1 \text{ eV}$ , we can see the QP peaks whose dc limits agree with the measured dc conductivity values, marked with symbols. As Ca replaces Sr, the QP peak decreases. In the frequency region of  $1 \sim 2 \text{ eV}$ , there are broad features of the  $U/2$  peaks. Around 3 eV, the  $U$  peaks can be seen with a very broad background absorption. [15] The background comes from a charge transfer excitation between  $\text{O}(2p)$  and  $\text{Ru}(4d)$  with an energy higher than  $U$ , [16] and its estimated contribution is indicated with the dashed-double-dotted line. Even with this charge transfer contribution, this spectral feature resembles quite closely to Fig. 1(b).

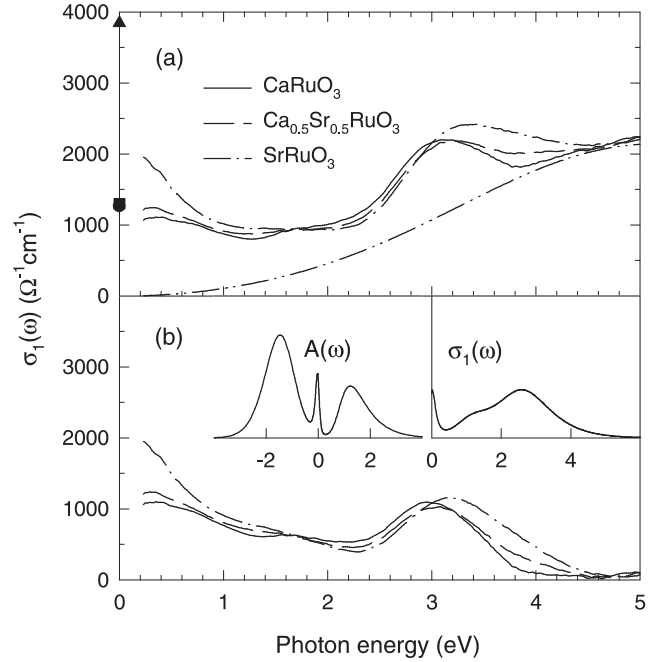


FIG. 3. (a) Optical conductivity spectra of  $(\text{Ca,Sr})\text{RuO}_3$  films at room temperature. Symbols indicate dc values obtained from dc measurements. ( $\blacktriangle$ :  $\text{SrRuO}_3$ ,  $\blacksquare$ :  $\text{Ca}_{0.5}\text{Sr}_{0.5}\text{RuO}_3$ , and  $\bullet$ :  $\text{CaRuO}_3$ ) Dashed-double-dotted line shows the charge transfer transition between  $\text{O}(2p)$  and  $\text{Ru}(4d)$ . [16] (b) Optical conductivity spectra after the charge transfer transition contribution is subtracted. Inset: single particle spectral function and optical conductivity calculated from a QMC simulation with  $U/W \sim 1.95$  for the  $4/6$ -filled triply degenerate orbitals.

Figure 3(b) shows  $\sigma_1(\omega)$  after the background absorption is subtracted. Note that the QP peaks are not changed very much after the subtraction. From these spectra,  $U$  and  $W$  are experimentally determined from the center and the half-width of the  $U$  peak: values of  $\{U, W\}$ , in the unit of eV, are  $\{2.99 \pm 0.05, 1.16 \pm 0.07\}$  for  $\text{CaRuO}_3$ ,  $\{3.07 \pm 0.05, 1.20 \pm 0.04\}$  for  $\text{Ca}_{0.5}\text{Sr}_{0.5}\text{RuO}_3$ , and  $\{3.23 \pm 0.05, 1.31 \pm 0.04\}$  for  $\text{SrRuO}_3$ . As Sr replaces Ca,  $U$  and  $W$  increase systematically, where the relative change in  $W$  is larger than that of  $U$ . Therefore, the  $(\text{Ca,Sr})\text{RuO}_3$  films can be considered effectively as a bandwidth controlled Mott-Hubbard system.

The broad feature of the QP peaks could be described with the extended Drude model, [17] which provides informations on frequency dependent mass  $m^*(\omega)$  and scattering rate  $1/\tau(\omega)$ . [18] As shown in Fig. 4, all of the samples showed mass enhancements as frequency becomes lowered. Values of  $m^*(\omega = 0)$ , i.e.  $m^*$ , determined by specific heat measurements, for  $\text{CaRuO}_3$  [8] and  $\text{SrRuO}_3$  [11] are marked with the open circle and triangle, respectively. Since the carrier concentration is fixed for the  $(\text{Ca,Sr})\text{RuO}_3$  films, the enhancement of  $m^*$  could be attributed to the correlation effect. As Ca replaces Sr,  $m^*$  becomes larger, indicating that  $\text{CaRuO}_3$  is more close to

the Mott M-I transition due to band narrowing. Similar behaviors were observed for (Sr,La)TiO<sub>3</sub>, which is a band filling controlled Mott-Hubbard system. [5] On the other hand, such a mass enhancement was not optically observed for (Ca,Sr)VO<sub>3</sub>, which is also considered as a bandwidth controlled system. [6] Inset in Fig. 4 shows spectra of  $1/\tau(\omega)$  for our (Ca,Sr)RuO<sub>3</sub> films. The frequency dependence is almost linear up to 1 eV and the slopes are nearly the same for all samples. This linear frequency dependence has been observed in many other correlated systems, [6,19] however, there is still no concrete explanation for this behavior.

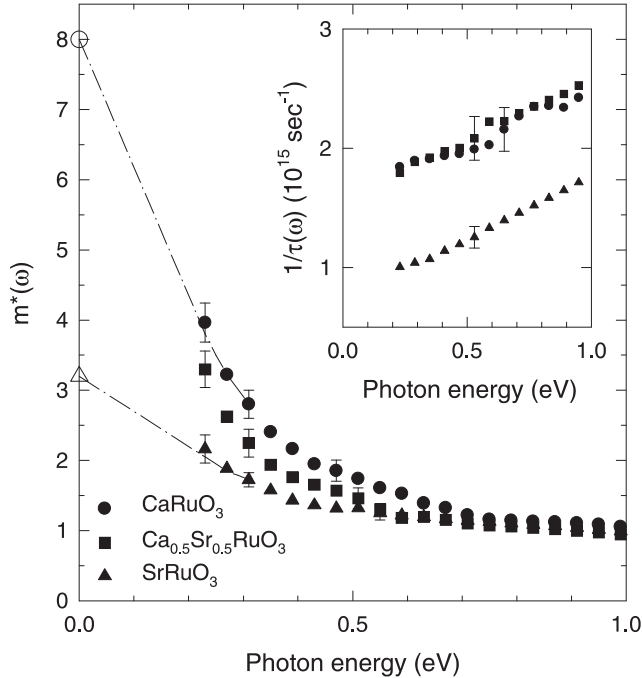


FIG. 4. Low energy mass enhancement  $m^*(\omega)$  obtained from optical data using the extended Drude model.  $m^*$ 's from specific heat measurements are shown with  $\circ$  (CaRuO<sub>3</sub>) [11] and  $\triangle$  (SrRuO<sub>3</sub>). [8] The dashed-dotted lines are guidelines for eye. Inset shows corresponding frequency dependent scattering rate,  $1/\tau(\omega)$ .

Within the GBR picture for the Mott transition, the spectral weight of the QP peak,  $\omega_p^{*2}$ , is an order parameter and should be proportional to  $1/m^*$ . Using a relation such that

$$\omega_p^{*2} \simeq 8 \int_0^{1 \text{ eV}} \sigma(\omega) d\omega, \quad (2)$$

$\omega_p^{*2}$  values for the (Ca,Sr)RuO<sub>3</sub> films could be estimated. As shown in Fig. 5(a), the measured values of  $\omega_p^{*2}$  are quite linear to  $1/m^*(\omega = 0.23 \text{ eV})$  with a very small y-axis intercept, demonstrating that most of free carriers in the (Ca,Sr)RuO<sub>3</sub> films are correlated QP's. Fig. 5(b) shows the dependence of  $(U/W)^2$  on  $1/m^*(\omega = 0.23 \text{ eV})$ . From Eq. (1),  $(U/W)^2$  should be proportional to

$(-1/m^*)$ , and the y-axis intercept should provide information on  $(U/W)_c$ . With  $m^*(\omega = 0.23 \text{ eV})$ ,  $(U/W)_c$  was estimated to be about 2.7. When we use dc values of  $m^*$ , which were shown with the open circle and triangle,  $(U/W)_c$  was estimated to be slightly lower by 0.05. It should be noted that the linear behaviors in Figs. 5(a) and 5(b) clearly demonstrate a self-consistency of our analysis based on the correlation picture.

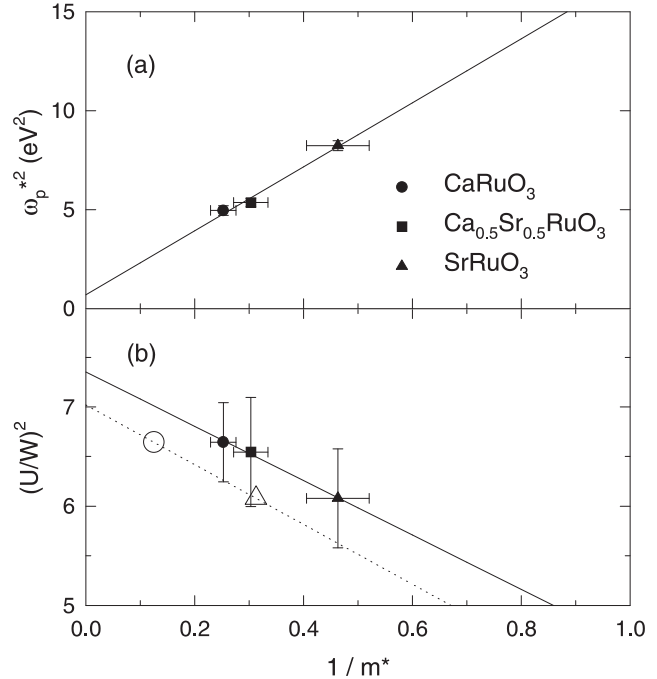


FIG. 5. (a) Spectral weight of the QP peak,  $\omega_p^{*2}$ , versus  $1/m^*$ . (b)  $(U/W)^2$  versus  $1/m^*$ . Solid symbols represent the estimated values of  $1/m^*$  at  $\omega = 0.23 \text{ eV}$ . For the open symbols, i.e.  $\circ$  (CaRuO<sub>3</sub>) and  $\triangle$  (SrRuO<sub>3</sub>), the dc values from specific heat measurements are used.

Note that the measured value of  $(U/W)_c \simeq 2.7$  for (Ca,Sr)RuO<sub>3</sub> is much larger than that of quantum Monte Carlo (QMC) simulation result, i.e. 1.5, for the half-filled single band Hubbard model. [2] Reported general trends are that the orbital degeneracy increases  $(U/W)_c$ , and that the electron filling away from the half-filling decreases  $(U/W)_c$ . [20] From our QMC simulations for triply degenerate cases, it was found that  $(U/W)_c \simeq 2.3$  for half-filling, 2.0 for 2/6- and 4/6-fillings, and 1.9 for 1/6- and 5/6-fillings. [21] Even after the orbital degeneracy and the filling factor are considered properly, the QMC result seems to be smaller than our experimental value. Some portion of this discrepancy might come from the uncertainty in  $W$ , experimentally deduced from the half width of  $\sim 3 \text{ eV}$  optical absorption band. A similar problem existed in the metallic  $3d$  (Ca,Sr)VO<sub>3</sub> cases, even though it was not clearly stated. [22]

The QMC result for 4/6-filling is shown in the inset of Fig. 3(b). It is clearly seen that the predicted width of

the QP peak in  $\sigma_1(\omega)$  is much narrower than the measured value. [23] More theoretical considerations are required to explain our results for QP peak and  $(U/W)_c$ . Also, in  $(\text{Ca,Sr})\text{RuO}_3$ , there might be other kind of interactions, including  $p$ - $d$  hybridization, impurity scattering, and magnetic fluctuation due to double-exchange interaction, etc. The interplay of such interactions with Mott-Hubbard physics might provide us some more insights to understand the discrepancy of  $(U/W)_c$ , and even to explain why correlation effects appear to be so strong in  $4d$  electrons of ruthenates.

In summary, we found that  $(\text{Ca,Sr})\text{RuO}_3$  is a  $4d$  metal compound which has strong electron correlation effects. Its optical spectra display systematic changes in the spectral characteristics predicted for a metallic Mott-Hubbard system.

This work was supported by the Ministry of Education through BSRI-97-2416 and by the Korea Science and Engineering Foundation (KOSEF) through the RCDAMP of Pusan National University. One of us (JB) was supported by the KOSEF through the Postdoctoral Fellowship Program.

---

[1] N. F. Mott, *Metal-Insulator Transitions* (Taylor & Francis, London, ed. 2, 1990); P. P. Edwards and C. N. R. Rao, Eds., *Metal-Insulator Transitions Revisited* (Taylor & Francis, London, 1995); A. Husmann, D. S. Jin, Y. V. zastavker, T. F. Rosenbaum, X. Yao, and J. M. Honig, *Science* **274**, 1874 (1996).

[2] A. Georges, G. Kotliar, W. Krauth, and M. J. Rozenberg, *Rev. Mod. Phys.* **68**, 13 (1996), and references therein.

[3] W. F. Brinkman and T. M. Rice, *Phys. Rev. B* **2**, 4302 (1970).

[4]  $m^*$  is normalized quantity with respect to band mass for an uncorrelated system.

[5] Y. Tokura, Y. Taguchi, Y. Okada, Y. Fujishima, T. Arima, K. Kumagai, and Y. Iye, *Phys. Rev. Lett.* **70**, 2126 (1993).

[6] H. Makino, I. H. Inoue, M. J. Rozenberg, I. Hase, Y. Aiura, and S. Onari, cond-mat/9801086, Los Alamos e-Print Archive at xxx.lanl.gov (1998).

[7] I. I. Majin and D. J. Singh, *Phys. Rev. B* **56**, 2556 (1997).

[8] G. Cao, S. McCall, M. Shepard, J. E. Crow, and R. P. Guertin, *Phys. Rev. B* **56**, 321 (1997).

[9] T. Katsufuji, M. Kasai, and Y. Tokura, *Phys. Rev. Lett.* **76**, 126 (1996).

[10] P. Kostic, Y. Okada, Z. Schlesinger, J. W. Reiner, L. Klein, A. Kapitulnik, T. H. Geballe, and M. R. Beasley, cond-mat/9804041, Los Alamos e-Print Archive at xxx.lanl.gov (1998).

[11] P. A. Cox, R. G. Egdell, J. B. Goodenough, A. Hamnett, and C. C. Naish, *J. Phys. C: Solid State Phys.* **16**, 6221 (1983).

[12] R. A. Rao, Q. Gan, C. B. Eom, R. J. Cava, Y. Suzuki, J. J. Krajewski, S. C. Gausepohl, and M. Lee, *Appl. Phys. Lett.* **70**, 3035 (1997); C. B. Eom, R. J. Cava, R. M. Fleming, J. M. Philips, R. B. van Dover, J. H. Marshall, J. W. P. Hsu, J. J. Krajewski, and W. F. Peck, Jr., *Science* **258**, 1766 (1992).

[13] H. S. Choi, J. Bak, J. S. Ahn, N. J. Hur, T. W. Noh, and C. H. Cho, *J. Korean Phys. Soc.* **33** (1998), in press.

[14] K. H. Kim, J. Y. Gu, H. S. Choi, G. W. Park, and T. W. Noh, *Phys. Rev. Lett.* **77**, 1877 (1996).

[15]  $U \sim 3$  eV is reported from photoelectron studies of  $\text{SrRuO}_3$ . See K. Fujioka, J. Okamoto, T. Mizokawa, A. Fujimori, I. Hase, M. Abbate, H. J. Lin, C. T. Chen, Y. Takeda, and M. Makino, *Phys. Rev. B* **56**, 6380 (1997).

[16] From previous results, [11,15] we estimated the charge transfer excitation between  $\text{O}(2p)$  and  $\text{Ru}(4d)$  as a single Lorentzian peak, whose center and width are 5 and 6 eV, respectively.

[17] B. C. Webb, A. J. Sievers, and T. Mihalisin, *Phys. Rev. Lett.* **57**, 1951 (1986).

[18] For the calculation, plasma frequency  $\omega_p = 3.9$  eV is used.

[19] Z. Schlesinger *et al.*, *Phys. Rev. Lett.* **65**, 801 (1990).

[20] J. P. Lu, *Phys. Rev. B* **49**, 5687 (1994); O. Gunnarsson, E. Koch, and R. M. Martin, *Phys. Rev. B* **54**, R11026 (1996).

[21] On the other hand, 3.65 is obtained by Lu [20] from the analytical calculations for 4/6-filled triply degenerate case, within the Gutzwiller approximation.

[22] M. J. Rozenberg, I. H. Inoue, H. Makino, F. Iga, and Y. Nishihara, *Phys. Rev. Lett.* **76**, 4781 (1996).

[23] For the calculation, we used the dynamic mean field theory with  $T = 1/12$  (in the unit of  $W/2 = 1$ ).